THIELE CENTRE
FOR APPLIED MATHEMATICS IN NATURAL SCIENCE

Bayesian image restoration, using configurations

T. L. Thorarinsdottir

Research Report

No. 08 I June 2006

Bayesian image restoration, using configurations

This Thiele Research Report is also Research Report number 477 in the Stochastics Series at Department of Mathematical Sciences, University of Aarhus, Denmark.

Bayesian image restoration, using configurations

T.L. Thorarinsdottir*,†

Abstract

In this paper, we develop a Bayesian procedure for removing noise from images that can be viewed as noisy realisations of random sets in the plane. The procedure utilises recent advances in configuration theory for noise free random sets, where the probabilities of observing the different boundary configurations are expressed in terms of the mean normal measure of the random set. These probabilities are used as prior probabilities in a Bayesian image restoration approach. Estimation of the remaining parameters in the model is outlined for salt and pepper noise. The inference in the model is discussed in detail for 3×3 and 5×5 configurations and examples of the performance of the procedure are given.

1 Introduction

The comparison of neighbouring grid points in a discrete realisation of a random closed set Z in $\mathbb{R}^2$ has been used for decades to make inference on various characteristics of the random set. A classical result, cf. Serra (1982), states that the information obtained by comparing pairs of neighbouring grid points can be used to estimate the mean length of the total projection of the boundary of the random set in directions associated with the digitisation. This, in turn, yields certain information about the directional properties of the boundary. Larger configurations, such as grid squares of size 2×2 or 3×3, were used in Ohser *et al.* (1998) and Ohser and Mücklich (2000) to estimate the area density, length density, and density of the Euler number of Z.

In Jensen and Kiderlen (2003) and Kiderlen and Jensen (2003), the authors use grid squares of size $n \times n$, $n \geq 2$, to estimate the mean normal measure of the random set Z. The knowledge of this can then be used to quantify the anisotropy of Z. Events of type $tB \subset Z$, $tW \subset \mathbb{R}^2 \setminus Z$ are observed, where tB and tW are finite subsets of the scaled standard grid $t\mathbb{Z}^2$. The probability of such events,

$$\mathbb{P}(tB \subset Z, tW \subset \mathbb{R}^2 \setminus Z),$$

can effectively be estimated by filtering the discrete image. In digitised images, B usually stands for "black" points and W for "white" points. Here, we use the notion point for the mid-point of a pixel in the digitised image. We will not distinguish between a pixel and its mid-point and we use both notions in the following.

Another interesting aspect in the analysis of discrete planar random sets is the restoration of the random set from a noisy image. If the mean normal measure of the random set

*The T.N. Thiele Centre, Department of Mathematical Sciences, University of Aarhus
†The MR Research Centre, Skejby University Hospital, University of Aarhus

Z is known, the method in Kiderlen and Jensen (2003) and Jensen and Kiderlen (2003) can be reversed to obtain the prior probabilities for a Bayesian restoration procedure. The fundaments for Bayesian image analysis were developed by Ulf Grenander, see Grenander (1981), while the method itself was developed and popularised mainly by Geman and Geman (1984). For further readings on the subject, see e.g. Winkler (1995).

Hartvig and Jensen (2000a) introduce a spatial mixture modelling approach to the Bayesian image restoration. They consider $n \times n$ neighbourhoods around each pixel in the image, where $n \geq 3$ is an odd number. The prior probability of a certain constellation or pattern to be observed in the neighbourhood then depends on the number of black points in the given constellation. In other words, every two constellations with equal number of black points have the same prior probability. If, however, the restored image represents a random closed set Z that fulfils some regularity conditions and the resolution of the image is "good enough", the following constellations should not have equal prior probabilities:

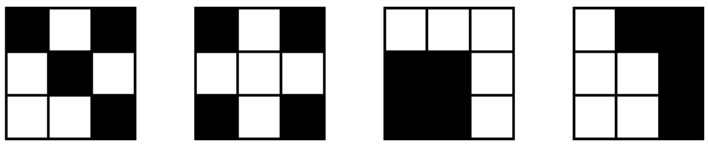

We use the theory from Jensen and Kiderlen (2003) and Kiderlen and Jensen (2003) to specify new prior probabilities for the spatial mixture model of Hartvig and Jensen (2000a). Here, a black and white constellation has a positive prior probability if and only if there exists a line going through the centre of at least two pixels that separates the black and the white points and hits only points of one colour.

The paper is organised as follows. Preliminaries concerning convex geometry, random sets, and image analysis are given in Section 2. The prior probabilities based on configuration theory are presented in Section 3. In Section 4, we specify the posterior probabilities for noisy images and discuss parameter estimation under the model. Three examples are given in Section 5. Finally, there are some concluding remarks in Section 6.

2 Preliminaries

A compact convex subset of $\mathbb{R}^2$ is called a *convex body* and we denote by $\mathcal{K}$ the family of convex bodies in $\mathbb{R}^2$. The *convex ring*, $\mathcal{R}$, is the family of finite unions of convex bodies while the *extended convex ring* is the family of all closed subsets $F \in \mathbb{R}^2$ such that $F \cap K \in \mathcal{R}$ for all $K \in \mathcal{K}$. Further, we denote by $L(K, \cdot)$ the *normal measure of* $K \in \mathcal{R}$ on the unit circle S^1. For a Borel set $A \in \mathcal{B}(S^1)$, $L(K, A)$ is the length of the part of the boundary of K with outer normal in A. L is thus a Borel measure on S^1 and the total mass $L(K, S^1)$ is just the boundary length $L(K)$ of K. The normal measure is sometimes called the first surface area measure and then denoted by $S^1(K, \cdot)$, cf. Schneider (1993, p. 214-218).

Now, let Z be a stationary random set in $\mathbb{R}^2$ with values in the extended convex ring. We assume in the following that Z satisfies the integrability condition

$$\mathbb{E}2^{N(Z \cap K)} < +\infty \tag{1}$$

for all $K \in \mathcal{K}$. Here, $N(U)$ is the minimal $k \in \mathbb{N}$ such that $U = \cup_{i=1}^{k} K_i$ with $K_i \in \mathcal{K}$ if $U \neq \emptyset$ and $N(\emptyset) = 0$. This condition is stricter than most standard integrability

conditions, but it guarantees that the realisations of Z do not become too complex in structure. The *mean normal measure* of Z is defined by

$$\bar{L}(Z,\cdot) = \lim_{r\to+\infty} \frac{\mathbb{E}L(Z\cap rK,\cdot)}{\nu_2(rK)},$$

where ν_2 is the Lebesgue measure on $\mathbb{R}^2$.

A digitisation (or discretisation) of Z is the intersection of Z with a scaled lattice. For a fixed scaling factor $t>0$, we consider $Z\cap t\mathbb{L}$, where

$$\mathbb{L} := \mathbb{Z}^2 = \{(i,j) : i,j\in\mathbb{Z}\}$$

is the usual lattice of points with integer coordinates. The lattice square

$$\mathbb{L}_n := \Big\{(i,j) : i,j = -\frac{n-1}{2},\dots,\frac{n-1}{2}\Big\}$$

consists of n^2 points ($n\geq 3, n$ odd). Here, we follow the notation in Hartvig and Jensen (2000a) and place the lattice square around a centre pixel. As we only consider lattice squares with odd number of points, this should not cause any conflicts in the notation. A line passing through at least two points of $\mathbb{L}_n$ will be called an *n-lattice line*.

Let $X\subset t\mathbb{Z}^2$ be a finite set and $t>0$. A binary image on X is a function $f: X\to\{0,1\}$. Here, f is given by $f(x)=\mathbb{1}\{x\in Z\}$ so that f is a random function due to the randomness of the set Z. We call a certain pattern of the values of f on a $n\times n$ grid a *configuration*. We denote it by C_t^n, where $t>0$ is the resolution of the grid, as in the definition of a lattice above. The elements of the configuration are numbered to match the numbering of the elements in the lattice square $\mathbb{L}_n$. For $n=3$ this gives

$$C_t^3 = \begin{bmatrix} c_{-1,1} & c_{0,1} & c_{1,1} \\ c_{-1,0} & c_{0,0} & c_{1,0} \\ c_{-1,-1} & c_{0,-1} & c_{1,-1} \end{bmatrix}_t,$$

and similarly for other allowed values of n. If the size of the configuration is clear from the context, we will omit the index n. Examples of 3×3 configurations are

$$\begin{bmatrix} \bullet & \circ & \circ \\ \bullet & \circ & \circ \\ \bullet & \bullet & \circ \end{bmatrix}_t \quad \begin{bmatrix} \bullet & \circ & \circ \\ \bullet & \circ & \bullet \\ \bullet & \bullet & \circ \end{bmatrix}_t \quad \begin{bmatrix} \circ & \bullet & \bullet \\ \bullet & \circ & \bullet \\ \bullet & \bullet & \circ \end{bmatrix}_t$$

where $\bullet$ means that $f(x)=1$ or equivalently $z\cap x\neq\emptyset$, while $\circ$ means that $f(x)=0$ or equivalently $z\cap x=\emptyset$. Here, z is the realisation of the random set Z observed in the image f.

3 Configuration probabilities

Let $f: X\to\{0,1\}$ be an image as before and let Z be a stationary random set that fulfils (1). In Kiderlen and Jensen (2003), the authors show that for $n>0$, a given $x\in X$, and a given configuration C_t,

$$\lim_{t\to 0^+}\frac{1}{t}\mathbb{P}\big(Z\cap t(\mathbb{L}_n+x)=C_t\big) = \int_{S^1} h(-v)\bar{L}(Z,dv). \tag{2}$$

The function h is given by

$$h(\cdot) = \big[\min_{x\in B}\langle x,\cdot\rangle - \max_{x\in W}\langle x,\cdot\rangle\big]^+,$$

where $(tB, tW) = C_t$ is the partitioning of the configuration C_t in "black" and "white" points, that is, $tB \subset Z$ and $tW \subset \mathbb{R}^2 \setminus Z$. Here, $g^+ := \max\{g, 0\}$ denotes the positive part of the function g and $\langle x, y\rangle$ denotes the usual inner product of the vectors x and y. A configuration C_t with non-identically zero h is called an *informative configuration*. C_t is informative if and only if there exists a n-lattice line separating tB and tW not hitting both of them. More precisely, $C_t = (tB, tW)$ is informative if and only if there exists an n-lattice line g such that tB is on one side of g, tW is on the other side of g and all the lattice points on g are either all black or all white.

Furthermore, it is shown in Jensen and Kiderlen (2003) that for a given informative configuration C_t, there exist vectors $a, b \in \mathbb{R}^2$ such that

$$h(-v) = \min\{\langle a, v\rangle^+, \langle b, v\rangle^+\}$$

for all $v \in S^1$. These results are then used to obtain estimators for the mean normal measure $\bar{L}(Z, \cdot)$ based on observed frequencies of the different types of configurations. If we, on the other hand, assume we have a discrete noisy image in $\mathbb{R}^2$, where the underlying image is a realisation of a stationary random closed set Z with a known mean normal measure $L(Z, \cdot)$, (2) provides prior probabilities in a Bayesian restoration procedure.

As an example, let us assume that Z is isotropic. Then, the mean normal measure $\bar{L}(Z, \cdot)$ is, up to a positive constant of proportionality, the Lebesgue measure on $[0, 2\pi)$. Equation (2) thus becomes

$$\begin{aligned}\lim_{t\to 0^+} \frac{1}{t}\mathbb{P}\big(Z \cap t(\mathbb{L}_n + x) = C_t\big) \\ = k \int_0^{2\pi} \min\big\{\langle a, (\cos\theta, \sin\theta)\rangle^+, \langle b, (\cos\theta, \sin\theta)\rangle^+\big\} d\theta, \end{aligned} \tag{3}$$

where $k > 0$ is a constant. For $t > 0$ small enough, such that only informative, all black, and all white configurations have positive probability, this gives the marginal probability of each informative configurations up to a constant of proportionality.

For $n = 3$, the vectors a and b are given in Jensen and Kiderlen (2003). We can thus insert those values without further effort into the right hand side of (3). For $x \in X$, this gives

$$\mathbb{P}\big(Z \cap (t\mathbb{L}_3 + x) = C_t\big) = \begin{cases} p_0, & C_t = \left[\begin{smallmatrix}\circ&\circ&\circ\\ \circ&\circ&\circ\\ \circ&\circ&\circ\end{smallmatrix}\right]_t \\ p_1, & C_t = \left[\begin{smallmatrix}\bullet&\bullet&\bullet\\ \bullet&\bullet&\bullet\\ \bullet&\bullet&\bullet\end{smallmatrix}\right]_t \\ p_2, & C_t \in R\Big(\left[\begin{smallmatrix}\bullet&\circ&\circ\\ \bullet&\circ&\circ\\ \bullet&\circ&\circ\end{smallmatrix}\right]_t, \left[\begin{smallmatrix}\bullet&\bullet&\circ\\ \bullet&\bullet&\circ\\ \bullet&\bullet&\circ\end{smallmatrix}\right]_t\Big) \\ p_3, & C_t \in R\Big(\left[\begin{smallmatrix}\circ&\circ&\circ\\ \bullet&\circ&\circ\\ \bullet&\bullet&\circ\end{smallmatrix}\right]_t, \left[\begin{smallmatrix}\bullet&\circ&\circ\\ \bullet&\bullet&\circ\\ \bullet&\bullet&\bullet\end{smallmatrix}\right]_t\Big) \\ p_4, & C_t \in R\Big(\left[\begin{smallmatrix}\bullet&\bullet&\circ\\ \bullet&\bullet&\bullet\\ \bullet&\bullet&\bullet\end{smallmatrix}\right]_t, \left[\begin{smallmatrix}\circ&\circ&\circ\\ \circ&\circ&\circ\\ \bullet&\circ&\circ\end{smallmatrix}\right]_t\Big) \\ p_5, & C_t \in R\Big(\left[\begin{smallmatrix}\bullet&\circ&\circ\\ \bullet&\circ&\circ\\ \bullet&\bullet&\circ\end{smallmatrix}\right]_t, \left[\begin{smallmatrix}\bullet&\circ&\circ\\ \bullet&\bullet&\circ\\ \bullet&\bullet&\circ\end{smallmatrix}\right]_t, \left[\begin{smallmatrix}\bullet&\bullet&\circ\\ \bullet&\bullet&\bullet\\ \bullet&\bullet&\bullet\end{smallmatrix}\right]_t, \left[\begin{smallmatrix}\circ&\circ&\circ\\ \bullet&\circ&\circ\\ \bullet&\circ&\circ\end{smallmatrix}\right]_t\Big) \\ 0, & \text{otherwise,} \end{cases}$$

where $R(\cdot)$ is the set of all possible rotations and reflections. The probabilities $p_2, \ldots, p_5$

are determined from (3) up to a multiplicative constant c. They are given by

$$\begin{aligned}
p_2 &= c\big[5\sin(\operatorname{atan}(2)) - 4\big],\\
p_3 &= c\big[5\sin(\operatorname{atan}(2)) - 3\sqrt{2}\big],\\
p_4 &= c\big[2 - \sqrt{2}\big],\\
p_5 &= c\big[1 + \sqrt{2} - \frac{5}{2}\sin(\operatorname{atan}(2))\big].
\end{aligned}$$

As the total probability is 1, we can express c in terms of the other unknown probabilities,

$$c = \frac{1 - p_0 - p_1}{16}.$$

For $n = 5$, we have used the methods described in Jensen and Kiderlen (2003) to determine the informative 5×5 configurations and the vectors a and b for each configuration. We have then calculated the prior probabilities in the same manner as described above for 3×3 configurations. The results from this can be found in Appendix A.

Knowledge of the mean normal measure of Z will not give us information about the probability of observing all white and all black configurations, as the mean normal measure is a property of the boundary of the set. The remaining parameters, p_0 and p_1 must thus be estimated from the data. This problem is treated in the next section.

4 Restoration of a noisy image

Let $F : X \to \{0, 1\}$ be a binary image on a finite set $X \subset t\mathbb{Z}^2$ for $t > 0$ and such that F can be viewed as a realisation of an isotropic stationary random set Z with noise. Note that the randomness in the image F is two-folded. First, the noise free image is random due to the randomness of the set Z. Second, a random noise is added to the image. By Bayes rule we have, for $x \in X$ and a given configuration C_t,

$$\begin{aligned}
&\mathbb{P}\big(Z \cap (t\mathbb{L}_n + x) = C_t | F(t\mathbb{L}_n + x)\big)\\
&\qquad \propto \mathbb{P}\big(Z \cap (t\mathbb{L}_n + x) = C_t\big) p\big(F(t\mathbb{L}_n + x) | Z \cap (t\mathbb{L}_n + x) = C_t\big).
\end{aligned}$$

We assume that $F(x_i)$ and $F(x_j)$ are conditionally independent given Z for all $x_i, x_j \in X$, and that the conditional distribution of $F(x)$ given Z only depends on $Z \cap x$ for all $x \in X$. Under these conditions, we get

$$p\big(F(t\mathbb{L}_n + x) | Z \cap (t\mathbb{L}_n + x) = C_t\big) = \prod_{k=1}^{n^2} p\big(F(y_k) | Z \cap y_k = c_k\big),$$

where $\{y_k\} = t\mathbb{L}_n + x$ and $\{c_k\} = C_t$.

By summing over the neighbouring states, we obtain the probability of Z hitting a single point $x \in X$,

$$\begin{aligned}
&\mathbb{P}\big(Z \cap x \neq \emptyset | F(t\mathbb{L}_n + x)\big)\\
&\qquad \propto \sum_{\{C_t : c_{00} = \bullet\}} \mathbb{P}\big(Z \cap (t\mathbb{L}_n + x) = C_t\big) \prod_{k=1}^{n^2} p\big(F(y_k) | Z \cap y_k = c_k\big) \qquad (4)\\
&=: S_1(x).
\end{aligned}$$

The probability of Z not hitting a single point $x \in X$ is obtained in a similar way. It is given by

$$\begin{aligned}
&\mathbb{P}\big(Z \cap x = \emptyset | F(t\mathbb{L}_n + x)\big) \\
&\qquad \propto \sum_{\{C_t : c_{00} = \circ\}} \mathbb{P}\big(Z \cap (t\mathbb{L}_n + x) = C_t\big) \prod_{k=1}^{n^2} p\big(F(y_k) | Z \cap y_k = c_k\big) \qquad (5) \\
&\qquad =: S_2(x).
\end{aligned}$$

As the probabilities in (4) and (5) sum to one, we only need to compare $S_1(x)$ and $S_2(x)$ for determining the restored value of the image for a pixel x. The restored value is 1 if $S_1(x) > S_2(x)$ and 0 otherwise.

To compare $S_1(x)$ and $S_2(x)$, we need to determine the densities $p\big(F(x)|Z \cap x\big)$ which depend on the distribution of the noise. As an example, we consider salt and pepper noise. That is, a black point is replaced by a white point with probability q, and vice versa. More precisely,

$$\begin{aligned}
p\big(F(x)|Z \cap x\big) = q^{F(x)}(1-q)^{1-F(x)} \ \ &\big\{Z \cap x = \emptyset\big\} \\
+ (1-q)^{F(x)} q^{1-F(x)} \ \ &\big\{Z \cap x \neq \emptyset\big\},
\end{aligned}$$

for some $0 \leq q \leq 1$. This noise model has one unknown parameter, q, which must be estimated from the data.

Further, we need to determine the marginal probability $\mathbb{P}\big(Z \cap (t\mathbb{L}_n + x) = C_t\big)$ of observing a given configuration, C_t. A method to obtain the prior probabilities of observing the different types of boundary configurations, that is configurations that contain both black and white points, is given in the previous section. We still lack information about the prior probabilities of observing configurations that are all black or all white, that is

$$p_0 = \mathbb{P}\Big(Z \cap (t\mathbb{L}_3 + x) = \Big[\begin{smallmatrix} \circ & \circ & \circ \\ \circ & \circ & \circ \\ \circ & \circ & \circ \end{smallmatrix}\Big]_t\Big)$$

and

$$p_1 = \mathbb{P}\Big(Z \cap (t\mathbb{L}_3 + x) = \Big[\begin{smallmatrix} \bullet & \bullet & \bullet \\ \bullet & \bullet & \bullet \\ \bullet & \bullet & \bullet \end{smallmatrix}\Big]_t\Big)$$

if $n = 3$ and similarly for larger n.

We use the parameter estimation approach introduced in Hartvig and Jensen (2000a) which is related to maximum likelihood estimation. Within the model, we can calculate the marginal density of an $n \times n$ neighbourhood. It is given by

$$\begin{aligned}
&p\big(F(t\mathbb{L}_n + x); p_0, p_1, q\big) \\
&\quad = \sum_{C_t} p\big(F(t\mathbb{L}_n + x) | Z \cap (t\mathbb{L}_n + x) = C_t; q\big) \mathbb{P}\big(Z \cap (t\mathbb{L}_n + x) = C_t; p_0, p_1\big) \\
&\quad = p_0 q^{\sum F(y_k)} (1-q)^{n^2 - \sum F(y_k)} + p_1 q^{n^2 - \sum F(y_k)} (1-q)^{\sum F(y_k)} \\
&\qquad + \frac{1 - p_0 - p_1}{A(n)} \sum_{C_t \text{ inform.}} B(C_t) \prod_{k=1}^{n^2} \big[q^{F(y_k)}(1-q)^{1-F(y_k)} \ \ \{Z \cap y_k = \emptyset\} \\
&\qquad\qquad + q^{1-F(y_k)}(1-q)^{F(y_k)} \ \ \{Z \cap y_k \neq \emptyset\}\big],
\end{aligned}$$

where the constant $B(C_t)$ is given by the integral on the right hand side of (3) and $A(n) = \sum_{C_t \text{ inform.}} B(C_t)$. We have $A(3) = 16$ and $A(5) = 32$.

A possibility for estimating the parameters p_0, p_1, and q is to maximise the contrast function

$$\gamma(p_0, p_1, q) = \sum_{x \in X} \log p\big(F(t\mathbb{L}_n + x); p_0, p_1, q\big). \tag{6}$$

This is, however, computationally a very demanding task. We have therefore used a simplified version of the approach. The probability that a single point $x \in X$ is in the set Z is

$$\begin{aligned}\mathbb{P}\big(Z \cap x \neq \emptyset\big) &= \sum_{\{C_t : c_{00} = \bullet\}} \mathbb{P}\big(Z \cap (t\mathbb{L}_n + x) = C_t\big) \\ &= \frac{1 - p_0 - p_1}{2} + p_1 \\ &= \frac{1 - p_0 + p_1}{2},\end{aligned}$$

as exactly half of the boundary configurations have a black mid-point. The marginal density of a single point is thus given by

$$\begin{aligned}&p\big(F(x); p_0, p_1, q\big) \\ &\quad = \mathbb{P}\big(Z \cap x \neq \emptyset; p_0, p_1\big) p\big(F(x) | Z \cap x \neq \emptyset; q\big) \\ &\qquad + \mathbb{P}\big(Z \cap x = \emptyset; p_0, p_1\big) p\big(F(x) | Z \cap x = \emptyset; q\big) \\ &\quad = \frac{1}{2}\Big[(1 - p_0 + p_1) q^{1 - F(x)} (1 - q)^{F(x)} + (1 + p_0 - p_1) q^{F(x)} (1 - q)^{1 - F(x)}\Big].\end{aligned}$$

The corresponding contrast function

$$\gamma_m(p_0, p_1, q) = \sum_{x \in X} \log p\big(F(x); p_0, p_1, q\big),$$

can easily be differentiated with repect to the parameters p_0, p_1, and q. The differentiation yields that the maximum of γ_m is obtained when

$$p_1 = p_0 + \frac{2 \sum F(x) - |X|}{|X|(1 - 2q)},$$

where $|X|$ denotes the number of points in X. In the examples in Section 5, we have inserted this into (6) and maximised γ on a grid with $q \in [0.05, 0.1, \ldots, 0.45, 0.49]$ and $p_0 \in [0.05, 0.1, \ldots, 0.9]$ under the constraints

$$2p_0 + \frac{2 \sum F(x) - |X|}{|X|(1 - 2q)} < 1, \qquad p_0 + \frac{2 \sum F(x) - |X|}{|X|(1 - 2q)} \geq 0.$$

5 Examples

We illustrate the method by applying it to two synthetic datasets and one real data set. We use the salt and pepper noise model and isotropic priors for the configuration probabilities in all three examples. The method can not be used directly to restore the values on the edge of an image. In the examples below, we have therefore a one-pixel-wide

edge of white (background) pixels in each restored image for $n = 3$ and a two-pixel-wide edge of white pixels in each restored image for $n = 5$. Another possibility here would be to add either a one-pixel-wide boundary of white pixels for $n = 3$, or a two-pixel-wide boundary of white pixels for $n = 5$, around the noisy image before restoration. This will, however, lead to a slight underestimate of black pixels on the edge. We will quantify the results by the classification error. The classification error is estimated as the percentage of misclassified pixels (either type I or type II errors). The results given for the classification error are based on those pixels from the interior of each image where there are no edge effects.

Example 1 (Boolean model with isotropic grains)**.** The first example is based on digitisation of a simulated Boolean model. Boolean models are widely used as simple geometric models for random sets. The simulation of a Boolean model is a two-step procedure. First, independent uniform points are simulated in a sampling window. Second, a random grain is attached to each point. The grains are independent from one another and from the points. In order to avoid edge effects, the sampling window must be larger than the target window. Here, the target window is the unit square and the grains are circular discs with random radii. The radius of each grain is a uniform number from the interval $[0.0375, 0.15]$. Figure 1 (left) shows a realisation of this model. We have then digitised the image with $t = 0.01$ which gives a resolution of 100×100. The digitised image is shown in Figure 1 (right).

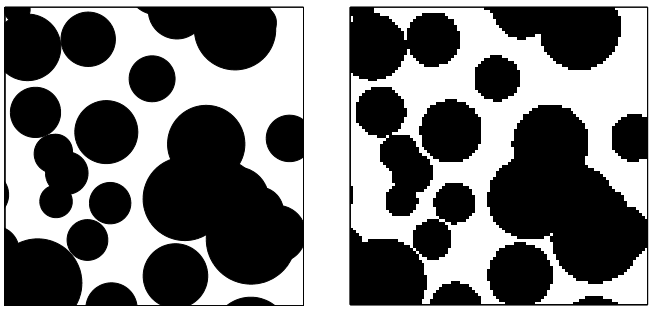

Figure 1: Boolean model with circular grains. Left: a realisation of the model on the unit square. Right: a digitised image of the realisation with resolution 100×100.

The digitised realisation of the Boolean model from Figure 1 (right) is now our original image. We have added salt and pepper noise to it for three different values of the noise parameter q. The noisy images are shown in Figure 2 (top row). In the leftmost image we have $q = 0.25$, in the middle image $q = 0.33$, and in the rightmost image $q = 0.4$. We have restored the original image from the noisy images using both 3×3 configurations and 5×5 configurations as described in the previous section. The resulting images for 3×3 configurations are shown in the middle row of Figure 2 and the resulting images for 5×5 configurations are shown in the bottom row of Figure 2. The parameter estimates and the classification errors for the restoration is shown in Table 1.

Example 2 (Boolean model with non-isotropic grains)**.** The grains in the Boolean model are here the right half of circular discs with random radii. The radius of each grain is a uniform number from the interval $[0.0375, 0.15]$ and the target window is again the unit square. A realisation of this model is shown in Figure 3 (left). As before, we have digitised

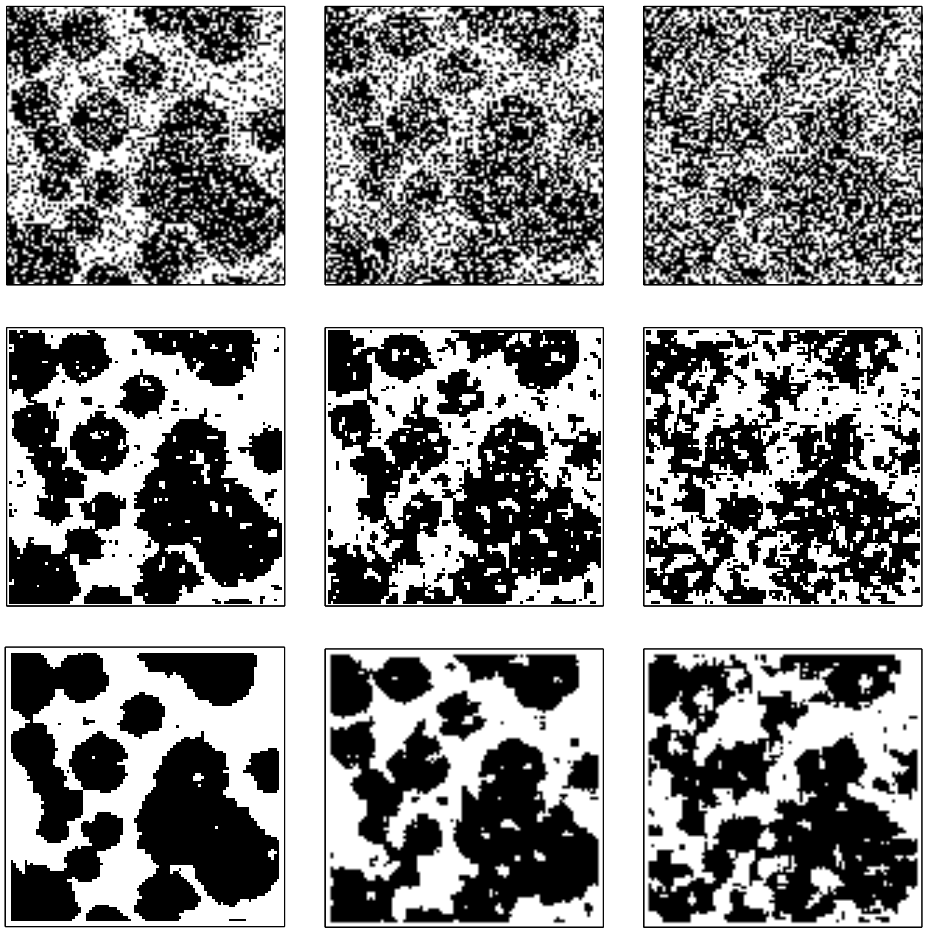

Figure 2: Restoration of the digitised realisation of the Boolean model with isotropic grains. Top row: the original image disturbed with salt and pepper noise for q equal to $0.25, 0.33$, and 0.4. Middle row: estimates of the true image using 3×3 configurations. Bottom row: estimates of the true image using 5×5 configurations.

Table 1: Parameter estimates, true parameter values, and classification errors for the restoration of a Boolean model with isotropic grains. The parameter estimates are based on five independent simulations of the degraded image. The standard errors of the estimates are given in parentheses. The classification errors are given in percentage.

$n \times n$	q	$\hat{q}$	p_0	$\hat{p}_0$	p_1	$\hat{p}_1$	Class. error
3×3	0.25	0.25 (0)	0.30	0.31 (0.02)	0.45	0.45 (0.01)	8.98 (0.55)
5×5	0.25	0.25 (0)	0.20	0.21 (0.02)	0.35	0.35 (0.01)	5.11 (0.39)
3×3	0.33	0.32 (0.03)	0.30	0.33 (0.08)	0.45	0.48 (0.10)	17.79 (0.01)
5×5	0.33	0.33 (0.03)	0.20	0.22 (0.07)	0.35	0.37 (0.09)	10.61 (0.32)
3×3	0.40	0.40 (0)	0.30	0.31 (0.08)	0.45	0.45 (0.06)	29.19 (0.77)
5×5	0.40	0.40 (0)	0.20	0.22 (0.06)	0.35	0.36 (0.05)	21.20 (1.02)

the image with $t = 0.01$ which gives a resolution of 100×100. The digitised image is shown in Figure 3 (right).

We have proceeded exactly as in the previous example. The noisy images are shown in Figure 4 (top row). In the leftmost image we have $q = 0.25$, in the middle image $q = 0.33$, and in rightmost image $q = 0.4$. The restored images for 3×3 configurations are shown

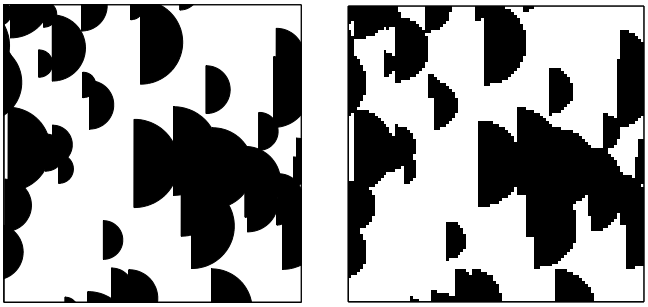

Figure 3: Boolean model with non-isotropic grains. Left: a realisation of the model on the unit square. Right: a digitised image of the realisation with resolution 100×100.

in the middle row of Figure 4 and the restored images for 5×5 configurations are shown in the bottom row of Figure 4. Further, Table 2 shows the parameter estimates and the classification errors for the restoration.

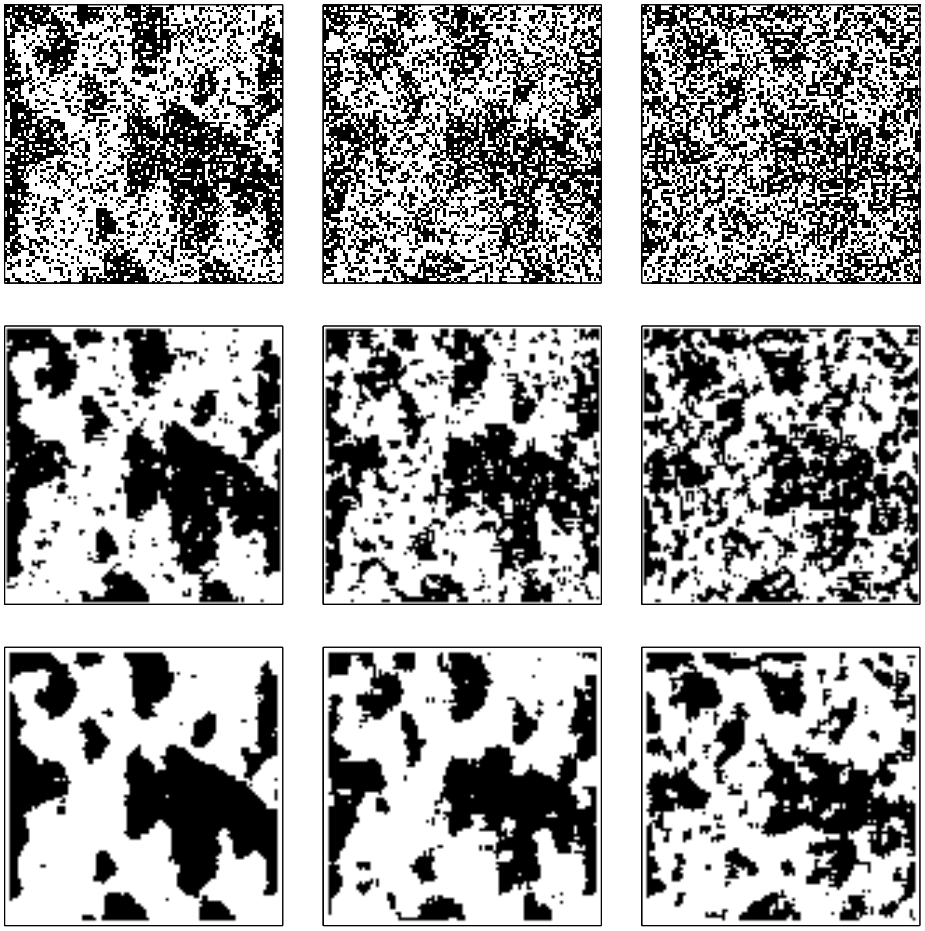

Figure 4: Restoration of the digitised realisation of the non-isotropic Boolean model. Top row: the original image disturbed with salt and pepper noise for q equal to $0.25, 0.33$, and 0.4. Middle row: estimates of the true image using 3×3 configurations. Bottom row: estimates of the true image using 5×5 configurations.

Example 3 (Image from steel data)**.** Our last example is an image showing the microstructure of steel. The image is from Ohser and Mücklich (2000), where it has been

Table 2: Parameter estimates, the true parameter values, and classification errors for the restoration of the non-isotropic Boolean model. The parameter estimates are based on five independent simulations of the degraded image. The standard errors of the estimates are given in parentheses. The classification errors are given in percentage.

$n \times n$	q	$\hat{q}$	p_0	$\hat{p}_0$	p_1	$\hat{p}_1$	Class. error
3×3	0.25	0.25 (0)	0.48	0.47 (0.03)	0.31	0.30 (0.03)	9.03 (0.15)
5×5	0.25	0.25 (0)	0.39	0.39 (0.02)	0.22	0.22 (0.01)	5.05 (0.29)
3×3	0.33	0.35 (0)	0.48	0.55 (0)	0.31	0.36 (0.02)	18.27 (0.88)
5×5	0.33	0.35 (0)	0.39	0.44 (0.02)	0.22	0.25 (0.03)	10.72 (0.60)
3×3	0.40	0.40 (0)	0.48	0.48 (0.03)	0.31	0.35 (0.04)	29.06 (0.52)
5×5	0.40	0.40 (0)	0.39	0.36 (0.04)	0.22	0.23 (0.04)	20.62 (0.74)

analysed to estimate the mean normal measure, see also Jensen and Kiderlen (2003). The thresholded, binary image of the data is shown in Figure 3. We have used Otsu's method for the thresholding. This method minimises the intraclass variance of the black and the white pixels, see Otsu (1979). The resolution of the image is 896×1280 pixels.

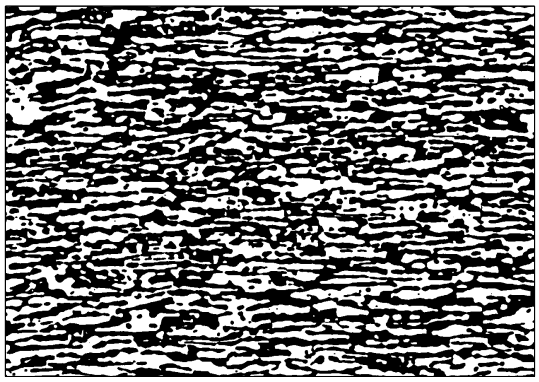

Figure 5: Binary image of rolled stainless steel in a longitudinal section. The light phase is ferrite, the black phase is austenite. From Osher and Mücklich (2000).

We have added salt and pepper noise to the binary image for $q = 0.25$ and $q = 0.33$. The noisy images can be seen in Figure 6 (top row). We have used the method described in the previous section for the restoration of the noisy images, using isotropic priors for the informative configurations. The resulting images can be seen in Figure 6 (middle row) for 3×3 configurations and in Figure 6 (bottom row) for 5×5 configurations. Further, the parameter estimates and the classification errors for the estimates are shown in Table 3.

6 Discussion

In the two first examples we have images of a similar type, the only difference is the mean normal measure of the boundary of the objects. In Example 1, the grains have isotropic boundaries which means that the model is using the correct prior probabilities for the configurations. In Example 2, on the other hand, there are some configurations that have

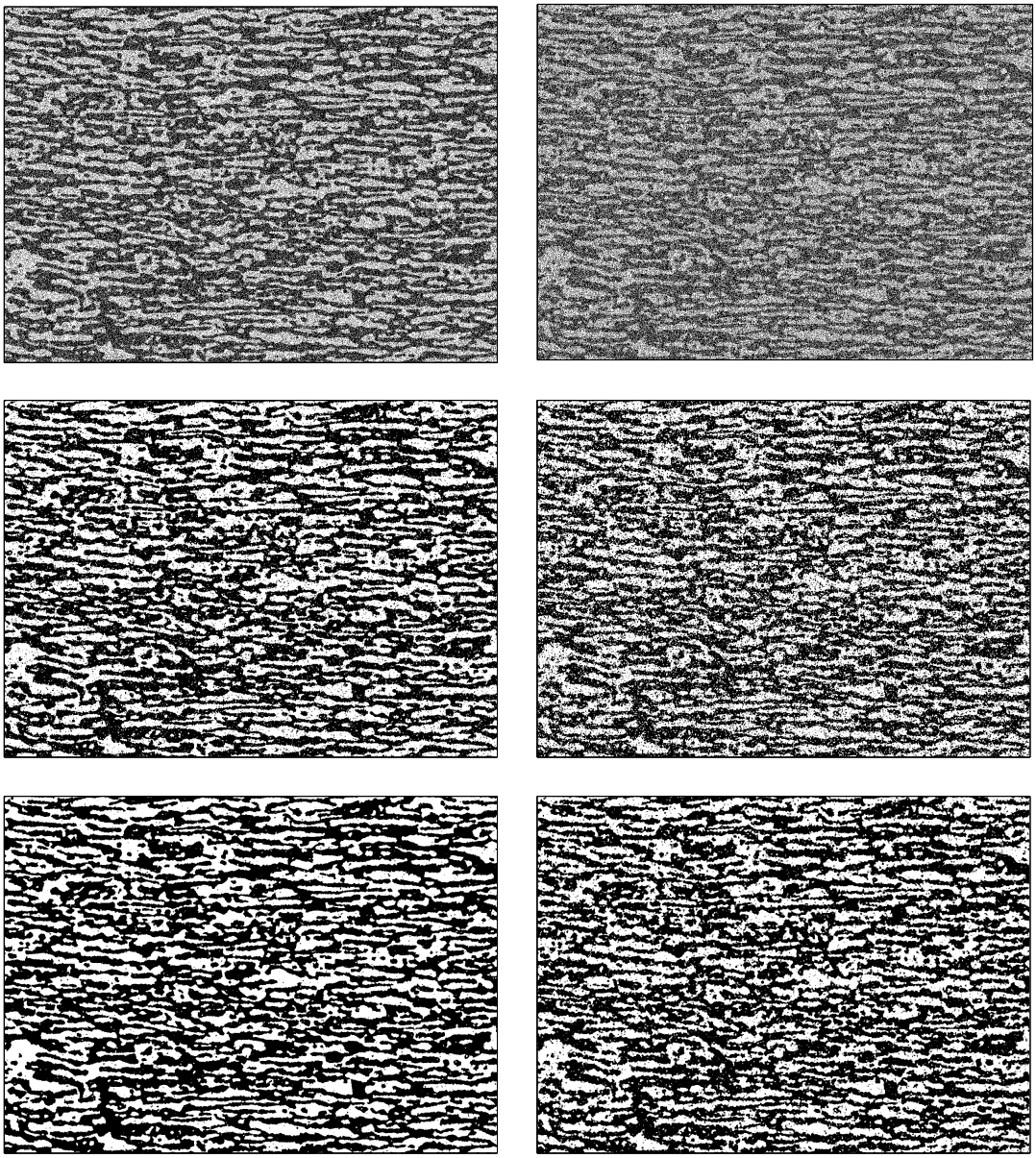

Figure 6: Restoration of the steel data image. Top row: the original binary image disturbed with salt and pepper noise for $q = 0.25$ (left) and $q = 0.33$ (right). Middle row: estimates of the true image using 3×3 configurations. Bottom row: estimates of the true image using 5×5 configurations.

Table 3: Parameter estimates, the true parameter values, and classification errors for the restoration of the steel data image. The parameter estimates are based on five independent simulations of the degraded image. The standard errors of the estimates are given in parentheses. The classification errors are given in percentage.

$n \times n$	q	$\hat{q}$	p_0	$\hat{p}_0$	p_1	$\hat{p}_1$	Class. error
3×3	0.25	0.25 (0)	0.34	0.35 (0)	0.45	0.46 (0.002)	8.92 (0.03)
5×5	0.25	0.25 (0)	0.25	0.25 (0)	0.35	0.36 (0.002)	4.90 (0.03)
3×3	0.33	0.35 (0)	0.34	0.40 (0)	0.45	0.53 (0.003)	17.74 (0.03)
5×5	0.33	0.35 (0)	0.25	0.30 (0)	0.35	0.43 (0.003)	10.71 (0.05)

much higher probability than suggested in the prior. The configurations

$$\left[\begin{smallmatrix}\circ & \bullet & \bullet\\ \circ & \bullet & \bullet\\ \circ & \bullet & \bullet\end{smallmatrix}\right]_t \text{ and } \left[\begin{smallmatrix}\circ & \circ & \bullet\\ \circ & \circ & \bullet\\ \circ & \circ & \bullet\end{smallmatrix}\right]_t$$

are, for instance, more likely to occur in the image than the configurations

$$\left[\begin{smallmatrix}\circ & \circ & \circ\\ \bullet & \bullet & \bullet\\ \bullet & \bullet & \bullet\end{smallmatrix}\right]_t \text{ and } \left[\begin{smallmatrix}\circ & \circ & \circ\\ \circ & \circ & \circ\\ \bullet & \bullet & \bullet\end{smallmatrix}\right]_t.$$

According to the isotropic prior, however, these configurations are all equaly likely to occur. If we compare the results in Table 1 and Table 2, we see that the classification error in Example 2 is very similar to the classification error in Example 1 for the same amount of noise and the same type of model. This suggests that it is not necessary to know the mean normal measure of the boundary of the object precisely for our model to perform in a close to optimal way.

It is also clear from the results in the previous section that the model using 5×5 configurations is superior to the model using 3×3 configurations. This is not surprising since the true images are quite regular with large patches of either black or white pixels. One might suspect that the model using 3×3 configurations would be more appropriate for images where the object Z consists of relatively small, disconnected components. Another consideration here is whether it is of interest to consider larger configurations than 5×5 configurations. As one can see from Appendix A, the model is already quite complicated if we use 5×5 configurations. We think, therefore, that it is computationally not feasible to consider larger configurations. Further, and maybe more importantly, very large configurations will tend to remove any finer details in the original image.

The model presented in this paper is very local in nature. The estimated restored value in a given pixel only depends on the image values in a small neighbourhood around that pixel. For this reason, there is no obvious way how to derive the joint posterior distribution over the entire image from the posterior distribution of the marginals in the small neighbourhoods and it is the former that is needed for estimating the unknown global parameters in the model. We have chosen to use the contrast function from Hartvig and Jensen (2000b), as this seems a sensible choice with a close relation to maximum likelihood estimation. As noted in Woolrich *et al.* (2005), the difference between the parameter estimates using this contrast function and those that could be obtained if the joint posterior were available is not known. Our method seems, however, not very sensitive towards small changes in the parameter estimates. We can also see from Table 1 - 3 that we get fairly good parameter estimates by maximising the contrast function if the noise in the image is moderate, especially for the larger image in Example 3. For higher levels of noise, the accuracy in the parameter estimates seems to depend on the accuracy of the prior for the informative configurations. Further, note that the noise parameter, q, is estimated very accurately if the correct value of the parameter is available on the grid. The accuracy of the remaining estimates of the prior probabilities of all black and all white configurations, p_0 and p_1, depends on how well the noise parameter is estimated. It might therefore be of interest to use a finer grid for the estimation of q.

Acknowledgements

The author would like to thank Eva B. Vedel Jensen and Markus Kiderlen for many fruitful discussions and useful suggestions. Also, many thanks to Lars Madsen for the help with some of the technical issues.

A Informative 5×5 configurations

Using the methods described in Jensen and Kiderlen (2003), we have constructed all informative 5×5 configurations and calculated the vectors a and b which are needed for the calculation of the prior probabilities of the configurations, see Section 3. The results are given in Table 4. We have omitted both the index for the resolution of the grid and the index for the size of the configuration to save space in the table.

In the examples in Section 5, we have used an isotropic prior for the boundary configurations. For $x \in X$, the prior probabilities for 5×5 configurations are in this case given by

$$\mathbb{P}\big(Z \cap (t\mathbb{L}_5 + x) = C_t\big) = \begin{cases} p_0, & C_t = \left[\begin{smallmatrix} \circ & \circ & \circ & \circ & \circ \\ \circ & \circ & \circ & \circ & \circ \\ \circ & \circ & \circ & \circ & \circ \\ \circ & \circ & \circ & \circ & \circ \\ \circ & \circ & \circ & \circ & \circ \end{smallmatrix}\right]_t \\ p_1, & C_t = \left[\begin{smallmatrix} \bullet & \bullet & \bullet & \bullet & \bullet \\ \bullet & \bullet & \bullet & \bullet & \bullet \\ \bullet & \bullet & \bullet & \bullet & \bullet \\ \bullet & \bullet & \bullet & \bullet & \bullet \\ \bullet & \bullet & \bullet & \bullet & \bullet \end{smallmatrix}\right]_t \\ p_2, & C_t \text{ in group nr. } 1, \ldots, 4 \\ p_3, & C_t \text{ in group nr. } 5, \ldots, 8 \\ p_4, & C_t \text{ in group nr. } 9, \ldots, 12 \\ p_5, & C_t \text{ in group nr. } 13, \ldots, 20 \\ p_6, & C_t \text{ in group nr. } 21, \ldots, 24 \\ p_7, & C_t \text{ in group nr. } 25, \ldots, 32 \\ p_8, & C_t \text{ in group nr. } 33, \ldots, 36 \\ p_9, & C_t \text{ in group nr. } 37, \ldots, 44 \\ p_{10}, & C_t \text{ in group nr. } 45, \ldots, 52 \\ p_{11}, & C_t \text{ in group nr. } 53, \ldots, 60 \\ p_{12}, & C_t \text{ in group nr. } 61, \ldots, 68 \\ p_{13}, & C_t \text{ in group nr. } 69, \ldots, 76 \\ p_{14}, & C_t \text{ in group nr. } 77, \ldots, 84 \\ p_{15}, & C_t \text{ in group nr. } 85, \ldots, 92 \\ 0, & \text{otherwise.} \end{cases}$$

The prior probabilities for the informative configurations are ordered in a decreasing order. They can be calculated up to a multiplicative constant c by inserting the vectors a and b in Table 4 into the right hand side of (3). The unknown constant c can be expressed in terms of p_0 and p_1 by

$$c = \frac{1 - p_0 - p_1}{32}.$$

Table 4: The 92 groups of informative 5×5 configurations.

No.	Config.	Twin	Config.	Twin	Config.	Twin	a	b
1	$\left[\begin{smallmatrix} \bullet & \bullet & \bullet & \bullet & \circ \\ \bullet & \bullet & \bullet & \bullet & \bullet \\ \bullet & \bullet & \bullet & \bullet & \bullet \\ \bullet & \bullet & \bullet & \bullet & \bullet \\ \bullet & \bullet & \bullet & \bullet & \bullet \end{smallmatrix}\right]$	$\left[\begin{smallmatrix} \circ & \circ & \circ & \circ & \circ \\ \circ & \circ & \circ & \circ & \circ \\ \circ & \circ & \circ & \circ & \circ \\ \circ & \circ & \circ & \circ & \circ \\ \bullet & \circ & \circ & \circ & \circ \end{smallmatrix}\right]$					$\begin{pmatrix} 1 \\ 0 \end{pmatrix}$	$\begin{pmatrix} 0 \\ -1 \end{pmatrix}$
2	$\left[\begin{smallmatrix} \circ & \bullet & \bullet & \bullet & \bullet \\ \bullet & \bullet & \bullet & \bullet & \bullet \\ \bullet & \bullet & \bullet & \bullet & \bullet \\ \bullet & \bullet & \bullet & \bullet & \bullet \\ \bullet & \bullet & \bullet & \bullet & \bullet \end{smallmatrix}\right]$	$\left[\begin{smallmatrix} \circ & \circ & \circ & \circ & \circ \\ \circ & \circ & \circ & \circ & \circ \\ \circ & \circ & \circ & \circ & \circ \\ \circ & \circ & \circ & \circ & \circ \\ \circ & \circ & \circ & \circ & \bullet \end{smallmatrix}\right]$					$\begin{pmatrix} 0 \\ -1 \end{pmatrix}$	$\begin{pmatrix} -1 \\ 0 \end{pmatrix}$

Table 4: The 92 groups of informative 5×5 configurations (continued).

No.	Config.	Twin	Config.	Twin	Config.	Twin	a	b
3	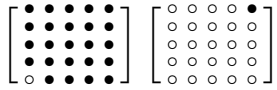						$\begin{pmatrix}0\\1\end{pmatrix}$	$\begin{pmatrix}-1\\0\end{pmatrix}$
4	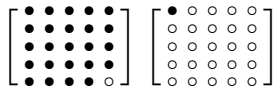						$\begin{pmatrix}1\\0\end{pmatrix}$	$\begin{pmatrix}0\\1\end{pmatrix}$
5	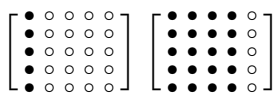		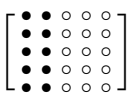	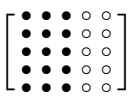			$\begin{pmatrix}1\\4\end{pmatrix}$	$\begin{pmatrix}1\\-4\end{pmatrix}$
6	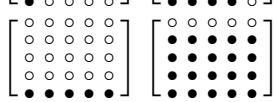		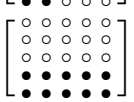	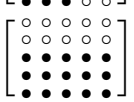			$\begin{pmatrix}4\\-1\end{pmatrix}$	$\begin{pmatrix}-4\\-1\end{pmatrix}$
7	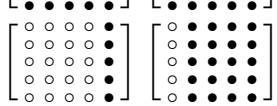		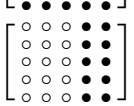	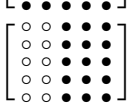			$\begin{pmatrix}-1\\4\end{pmatrix}$	$\begin{pmatrix}-1\\-4\end{pmatrix}$
8	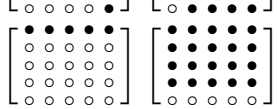		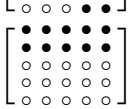	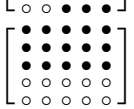			$\begin{pmatrix}4\\1\end{pmatrix}$	$\begin{pmatrix}-4\\1\end{pmatrix}$
9	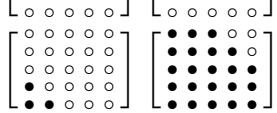						$\begin{pmatrix}2\\1\end{pmatrix}$	$\begin{pmatrix}-1\\-2\end{pmatrix}$
10	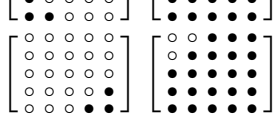						$\begin{pmatrix}1\\-2\end{pmatrix}$	$\begin{pmatrix}-2\\1\end{pmatrix}$
11	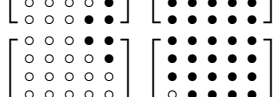						$\begin{pmatrix}1\\2\end{pmatrix}$	$\begin{pmatrix}-2\\-1\end{pmatrix}$
12	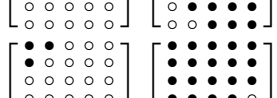						$\begin{pmatrix}2\\-1\end{pmatrix}$	$\begin{pmatrix}-1\\2\end{pmatrix}$
13	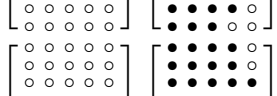						$\begin{pmatrix}1\\1\end{pmatrix}$	$\begin{pmatrix}0\\-1\end{pmatrix}$
14	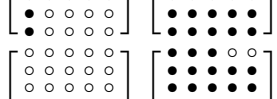						$\begin{pmatrix}1\\0\end{pmatrix}$	$\begin{pmatrix}-1\\-1\end{pmatrix}$
15	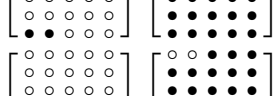						$\begin{pmatrix}1\\-1\end{pmatrix}$	$\begin{pmatrix}-1\\0\end{pmatrix}$
16	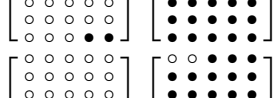						$\begin{pmatrix}0\\-1\end{pmatrix}$	$\begin{pmatrix}-1\\1\end{pmatrix}$
17	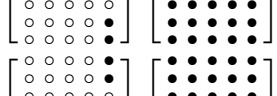						$\begin{pmatrix}0\\1\end{pmatrix}$	$\begin{pmatrix}-1\\-1\end{pmatrix}$
18	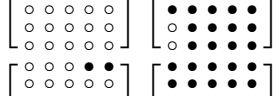						$\begin{pmatrix}1\\1\end{pmatrix}$	$\begin{pmatrix}-1\\0\end{pmatrix}$
19	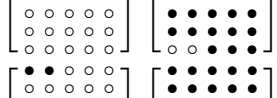						$\begin{pmatrix}1\\0\end{pmatrix}$	$\begin{pmatrix}-1\\1\end{pmatrix}$
20	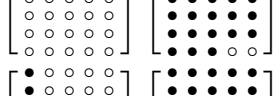						$\begin{pmatrix}1\\-1\end{pmatrix}$	$\begin{pmatrix}0\\1\end{pmatrix}$

Table 4: The 92 groups of informative 5×5 configurations (continued).

No.	Config.	Twin	Config.	Twin	Config.	Twin	a	b
21	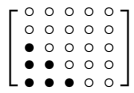	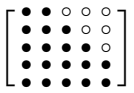					$\begin{pmatrix}3\\2\end{pmatrix}$	$\begin{pmatrix}-2\\-3\end{pmatrix}$
22	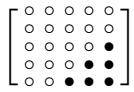	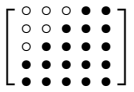					$\begin{pmatrix}2\\-3\end{pmatrix}$	$\begin{pmatrix}-3\\2\end{pmatrix}$
23	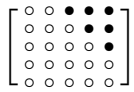	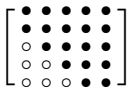					$\begin{pmatrix}2\\3\end{pmatrix}$	$\begin{pmatrix}-3\\-2\end{pmatrix}$
24	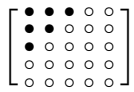	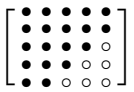					$\begin{pmatrix}3\\-2\end{pmatrix}$	$\begin{pmatrix}-2\\3\end{pmatrix}$
25	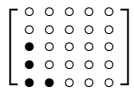	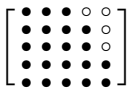					$\begin{pmatrix}1\\1\end{pmatrix}$	$\begin{pmatrix}-1\\-3\end{pmatrix}$
26	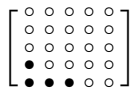	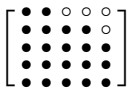					$\begin{pmatrix}3\\1\end{pmatrix}$	$\begin{pmatrix}-1\\-1\end{pmatrix}$
27	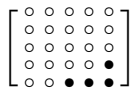	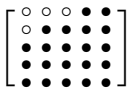					$\begin{pmatrix}1\\-1\end{pmatrix}$	$\begin{pmatrix}-3\\1\end{pmatrix}$
28	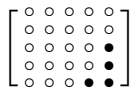	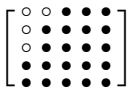					$\begin{pmatrix}1\\-3\end{pmatrix}$	$\begin{pmatrix}-1\\1\end{pmatrix}$
29	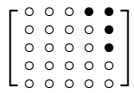	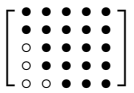					$\begin{pmatrix}1\\3\end{pmatrix}$	$\begin{pmatrix}-1\\-1\end{pmatrix}$
30	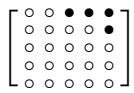	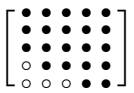					$\begin{pmatrix}1\\1\end{pmatrix}$	$\begin{pmatrix}-3\\-1\end{pmatrix}$
31	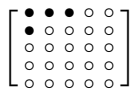	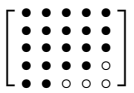					$\begin{pmatrix}3\\-1\end{pmatrix}$	$\begin{pmatrix}-1\\1\end{pmatrix}$
32	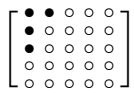	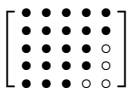					$\begin{pmatrix}1\\-1\end{pmatrix}$	$\begin{pmatrix}-1\\3\end{pmatrix}$
33	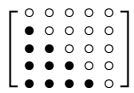	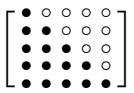					$\begin{pmatrix}4\\3\end{pmatrix}$	$\begin{pmatrix}-3\\-4\end{pmatrix}$
34	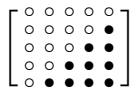	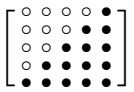					$\begin{pmatrix}3\\-4\end{pmatrix}$	$\begin{pmatrix}-4\\3\end{pmatrix}$
35	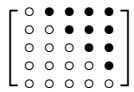	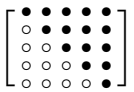					$\begin{pmatrix}3\\4\end{pmatrix}$	$\begin{pmatrix}-4\\-3\end{pmatrix}$
36	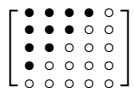	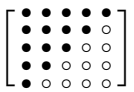					$\begin{pmatrix}4\\-3\end{pmatrix}$	$\begin{pmatrix}-3\\4\end{pmatrix}$
37	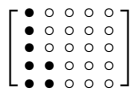	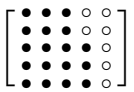	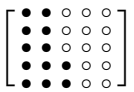	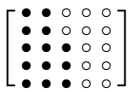	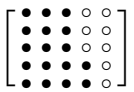	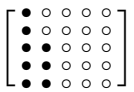	$\begin{pmatrix}1\\2\end{pmatrix}$	$\begin{pmatrix}0\\-1\end{pmatrix}$
	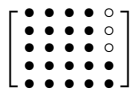	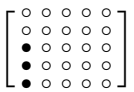						

Table 4: The 92 groups of informative 5×5 configurations (continued).

No.	Config.	Twin	Config.	Twin	Config.	Twin	a	b
38	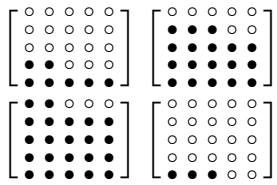	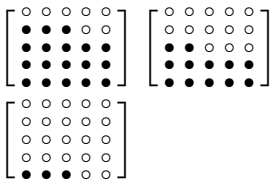	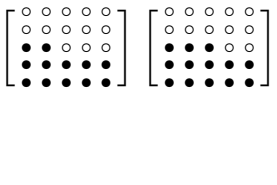	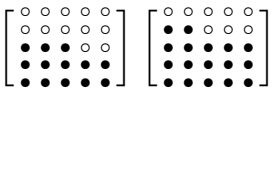	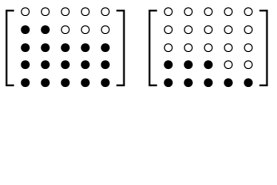	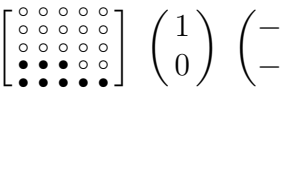	$\begin{pmatrix}1\\0\end{pmatrix}$	$\begin{pmatrix}-2\\-1\end{pmatrix}$
39	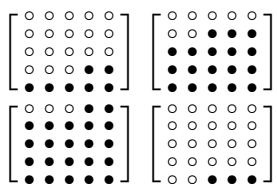	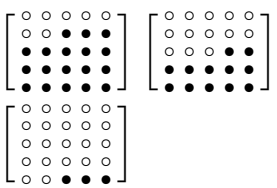	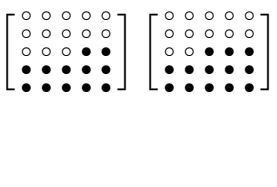	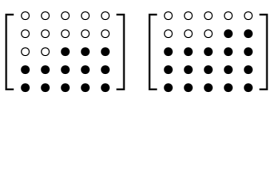	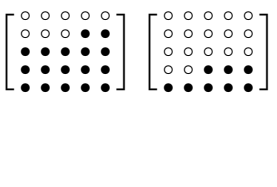	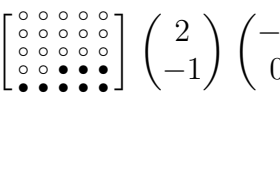	$\begin{pmatrix}2\\-1\end{pmatrix}$	$\begin{pmatrix}-1\\0\end{pmatrix}$
40	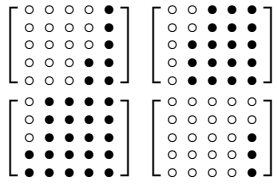	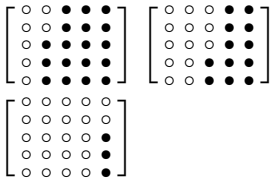	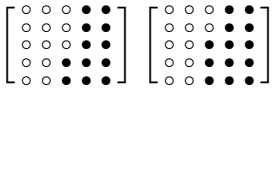	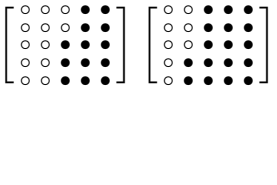	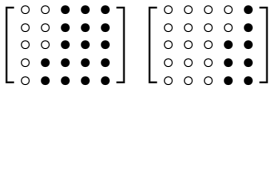	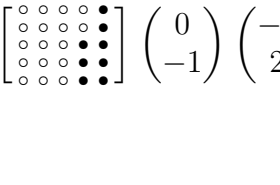	$\begin{pmatrix}0\\-1\end{pmatrix}$	$\begin{pmatrix}-1\\2\end{pmatrix}$
41	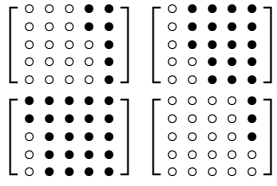	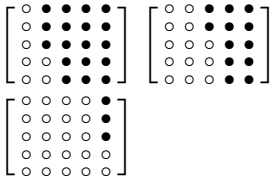	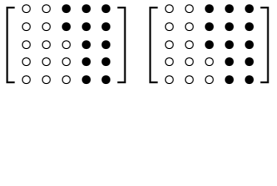	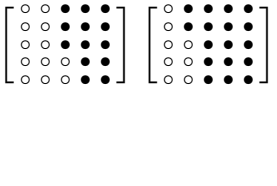	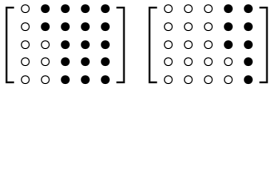	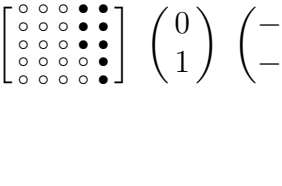	$\begin{pmatrix}0\\1\end{pmatrix}$	$\begin{pmatrix}-1\\-2\end{pmatrix}$
42	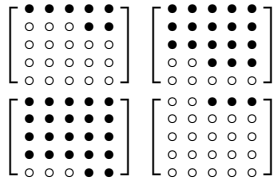	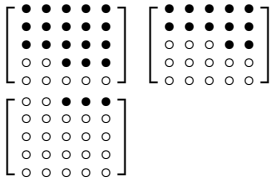	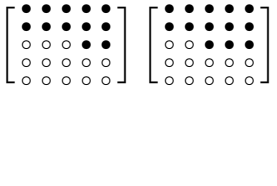	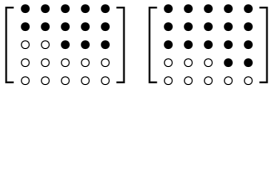	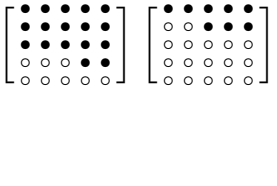	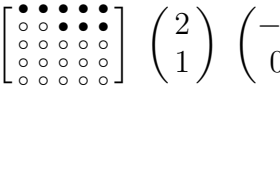	$\begin{pmatrix}2\\1\end{pmatrix}$	$\begin{pmatrix}-1\\0\end{pmatrix}$
43	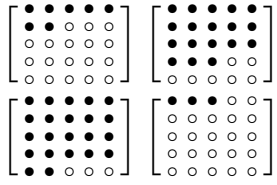	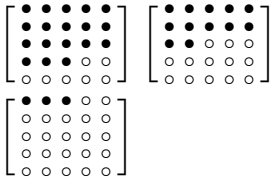	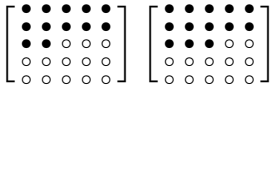	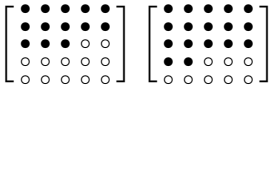	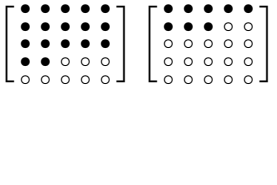	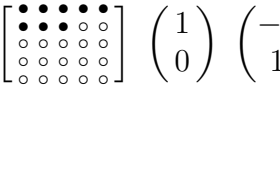	$\begin{pmatrix}1\\0\end{pmatrix}$	$\begin{pmatrix}-2\\1\end{pmatrix}$
44	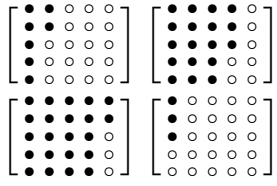	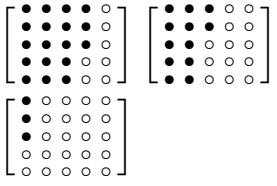	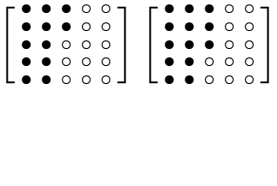	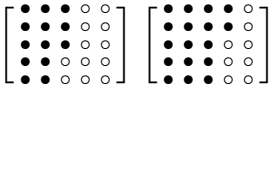	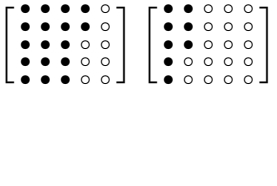	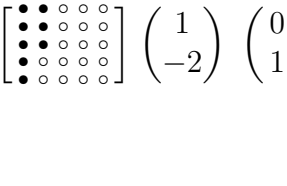	$\begin{pmatrix}1\\-2\end{pmatrix}$	$\begin{pmatrix}0\\1\end{pmatrix}$
45	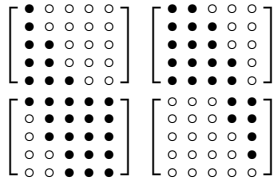	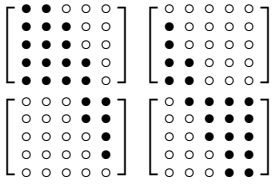	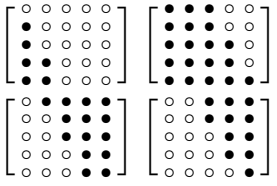	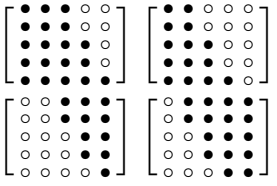	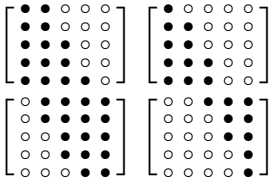	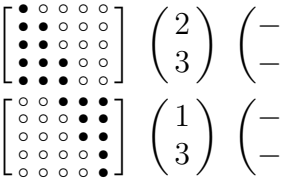	$\begin{pmatrix}2\\3\end{pmatrix}$	$\begin{pmatrix}-1\\-3\end{pmatrix}$
46	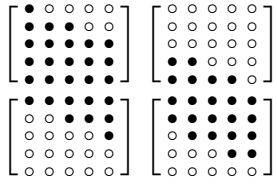	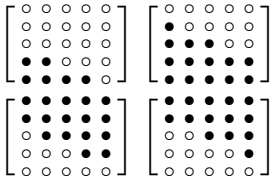	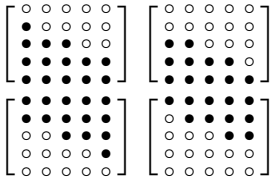	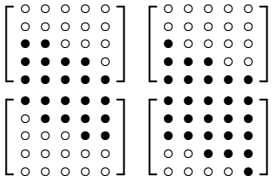	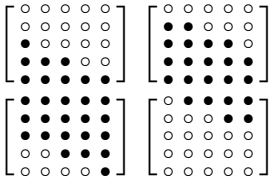	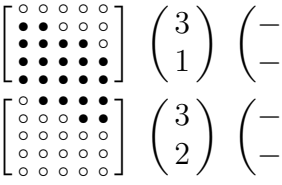	$\begin{pmatrix}1\\3\end{pmatrix}$	$\begin{pmatrix}-2\\-3\end{pmatrix}$
47			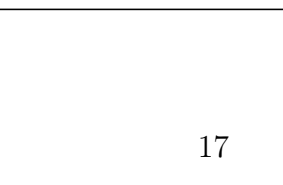				$\begin{pmatrix}3\\1\end{pmatrix}$	$\begin{pmatrix}-3\\-2\end{pmatrix}$
48							$\begin{pmatrix}3\\2\end{pmatrix}$	$\begin{pmatrix}-3\\-1\end{pmatrix}$

Table 4: The 92 groups of informative 5×5 configurations (continued).

No.	Config.	Twin	Config.	Twin	Config.	Twin	a	b
49	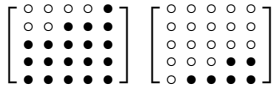		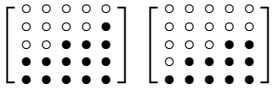		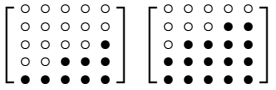		$\begin{pmatrix} 3 \\ -2 \end{pmatrix}$	$\begin{pmatrix} -3 \\ 1 \end{pmatrix}$
50	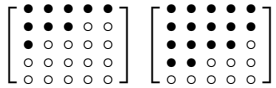		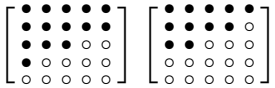		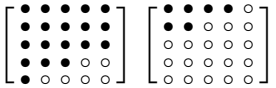		$\begin{pmatrix} 3 \\ -1 \end{pmatrix}$	$\begin{pmatrix} -3 \\ 2 \end{pmatrix}$
51	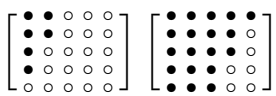		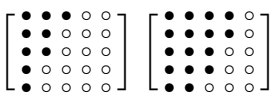		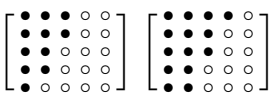		$\begin{pmatrix} 2 \\ -3 \end{pmatrix}$	$\begin{pmatrix} -1 \\ 3 \end{pmatrix}$
52	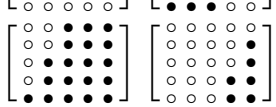		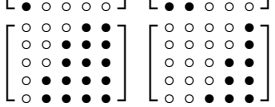		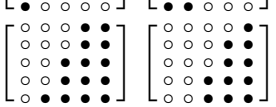		$\begin{pmatrix} 1 \\ -3 \end{pmatrix}$	$\begin{pmatrix} -2 \\ 3 \end{pmatrix}$
53	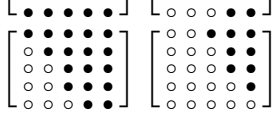		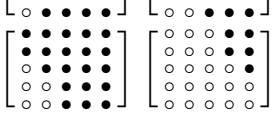		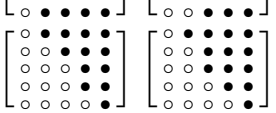		$\begin{pmatrix} 1 \\ 2 \end{pmatrix}$	$\begin{pmatrix} -1 \\ -1 \end{pmatrix}$
	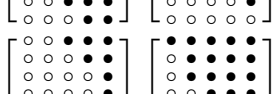							
54	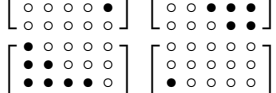		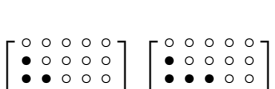		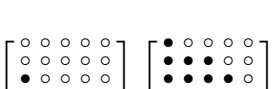		$\begin{pmatrix} 2 \\ 1 \end{pmatrix}$	$\begin{pmatrix} -1 \\ -1 \end{pmatrix}$
	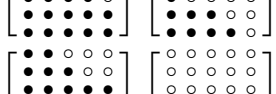							
55	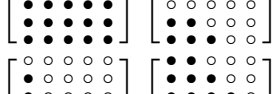		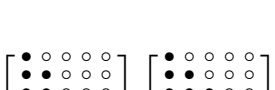		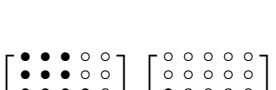		$\begin{pmatrix} 1 \\ 1 \end{pmatrix}$	$\begin{pmatrix} -1 \\ -2 \end{pmatrix}$
	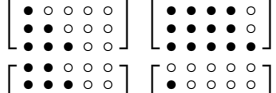							
56	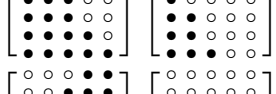		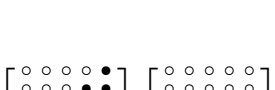		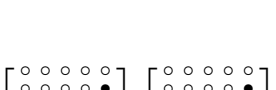		$\begin{pmatrix} 1 \\ -1 \end{pmatrix}$	$\begin{pmatrix} -2 \\ 1 \end{pmatrix}$
	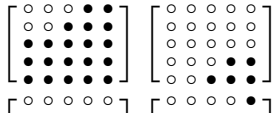							
57	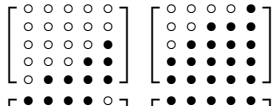						$\begin{pmatrix} 2 \\ -1 \end{pmatrix}$	$\begin{pmatrix} -1 \\ 1 \end{pmatrix}$
	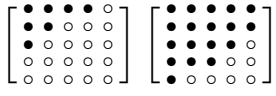							
58	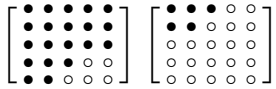						$\begin{pmatrix} 1 \\ 1 \end{pmatrix}$	$\begin{pmatrix} -2 \\ -1 \end{pmatrix}$
	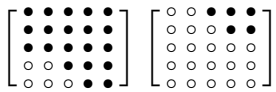							
59	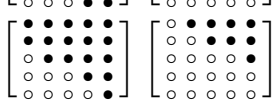						$\begin{pmatrix} 1 \\ -2 \end{pmatrix}$	$\begin{pmatrix} -1 \\ 1 \end{pmatrix}$
	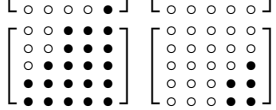							

Table 4: The 92 groups of informative 5×5 configurations (continued).

No.	Config.	Twin	Config.	Twin	Config.	Twin	a	b
60	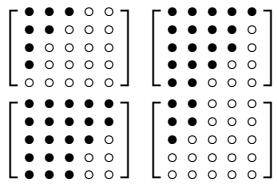		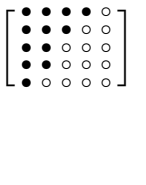	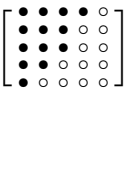	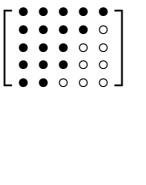	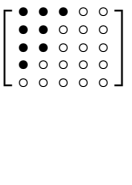	$\begin{pmatrix} 1 \\ -1 \end{pmatrix}$	$\begin{pmatrix} -1 \\ 2 \end{pmatrix}$
61	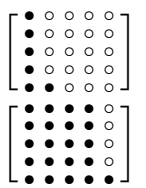	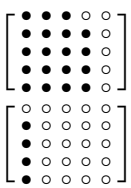	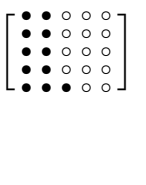	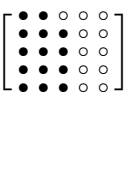	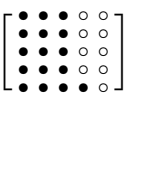	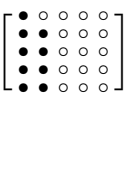	$\begin{pmatrix} 1 \\ 3 \end{pmatrix}$	$\begin{pmatrix} 0 \\ -1 \end{pmatrix}$
62	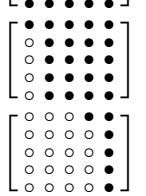	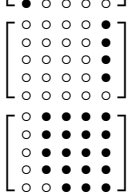	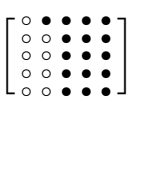	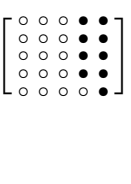	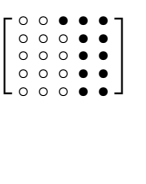	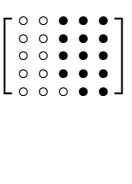	$\begin{pmatrix} 0 \\ 1 \end{pmatrix}$	$\begin{pmatrix} -1 \\ -3 \end{pmatrix}$
63	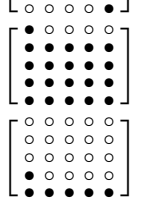	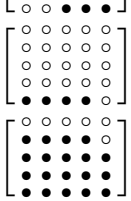	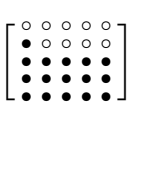	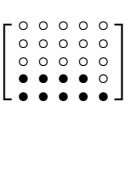	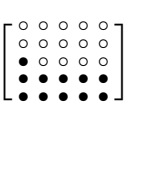	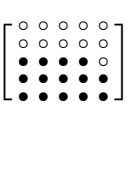	$\begin{pmatrix} 1 \\ 0 \end{pmatrix}$	$\begin{pmatrix} -3 \\ -1 \end{pmatrix}$
64	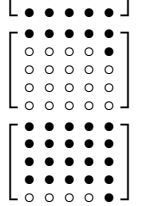	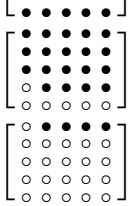	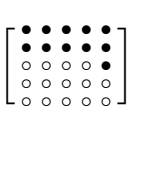	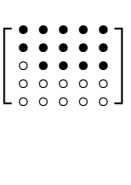	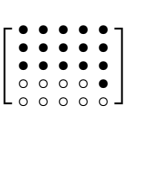	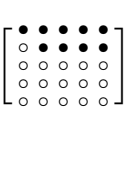	$\begin{pmatrix} 3 \\ 1 \end{pmatrix}$	$\begin{pmatrix} -1 \\ 0 \end{pmatrix}$
65	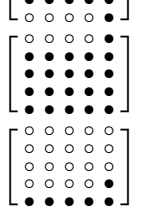	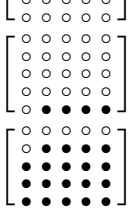	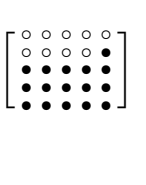	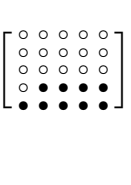	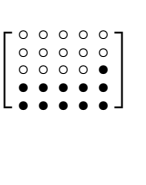	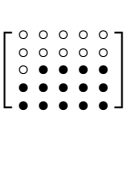	$\begin{pmatrix} 3 \\ -1 \end{pmatrix}$	$\begin{pmatrix} -1 \\ 0 \end{pmatrix}$
66	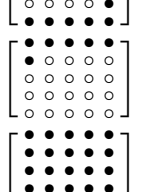	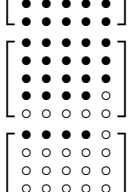	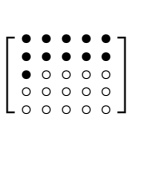	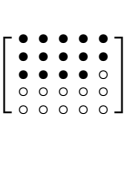	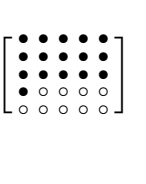	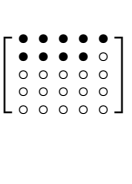	$\begin{pmatrix} 1 \\ 0 \end{pmatrix}$	$\begin{pmatrix} -3 \\ 1 \end{pmatrix}$
67	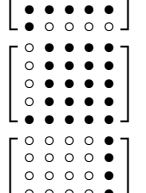	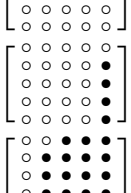	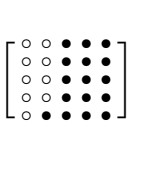	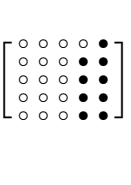	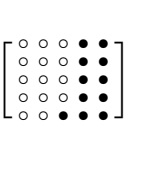	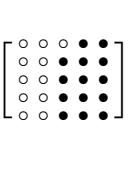	$\begin{pmatrix} 0 \\ -1 \end{pmatrix}$	$\begin{pmatrix} -1 \\ 3 \end{pmatrix}$
68	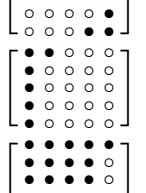	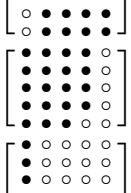	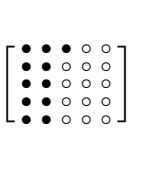	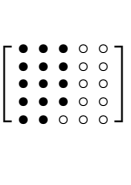	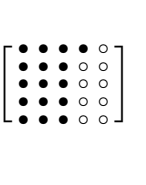	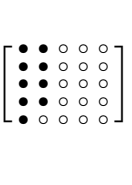	$\begin{pmatrix} 1 \\ -3 \end{pmatrix}$	$\begin{pmatrix} 0 \\ 1 \end{pmatrix}$

Table 4: The 92 groups of informative 5×5 configurations (continued).

No.	Config.	Twin	Config.	Twin	Config.	Twin	a	b
69	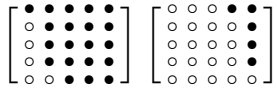		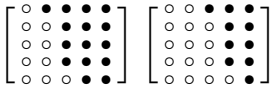				$\begin{pmatrix}1\\4\end{pmatrix}$	$\begin{pmatrix}-1\\-2\end{pmatrix}$
70	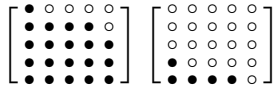		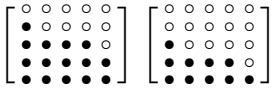				$\begin{pmatrix}4\\1\end{pmatrix}$	$\begin{pmatrix}-2\\-1\end{pmatrix}$
71	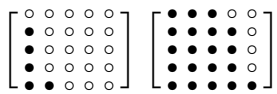		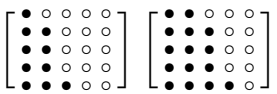				$\begin{pmatrix}1\\2\end{pmatrix}$	$\begin{pmatrix}-1\\-4\end{pmatrix}$
72	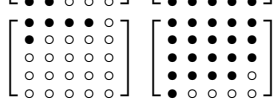		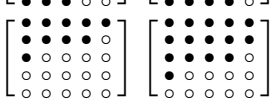				$\begin{pmatrix}4\\-1\end{pmatrix}$	$\begin{pmatrix}-2\\1\end{pmatrix}$
73	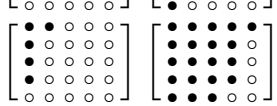		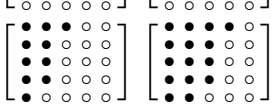				$\begin{pmatrix}1\\-2\end{pmatrix}$	$\begin{pmatrix}-1\\4\end{pmatrix}$
74	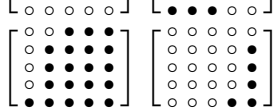		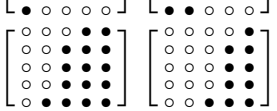				$\begin{pmatrix}1\\-4\end{pmatrix}$	$\begin{pmatrix}-1\\2\end{pmatrix}$
75	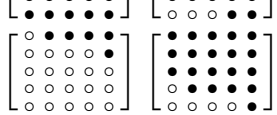		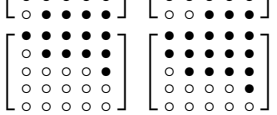				$\begin{pmatrix}2\\1\end{pmatrix}$	$\begin{pmatrix}-4\\-1\end{pmatrix}$
76	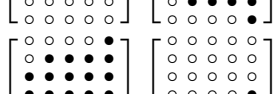		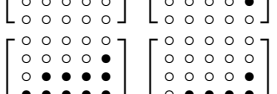				$\begin{pmatrix}2\\-1\end{pmatrix}$	$\begin{pmatrix}-4\\1\end{pmatrix}$
77	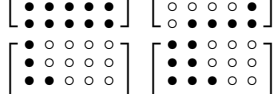						$\begin{pmatrix}3\\4\end{pmatrix}$	$\begin{pmatrix}-1\\-2\end{pmatrix}$
78	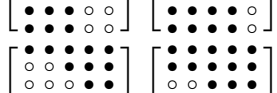						$\begin{pmatrix}4\\3\end{pmatrix}$	$\begin{pmatrix}-2\\-1\end{pmatrix}$
79	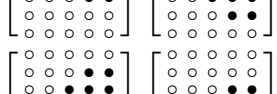						$\begin{pmatrix}4\\-3\end{pmatrix}$	$\begin{pmatrix}-2\\1\end{pmatrix}$
80	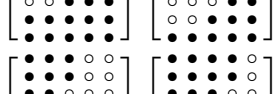						$\begin{pmatrix}3\\-4\end{pmatrix}$	$\begin{pmatrix}-1\\2\end{pmatrix}$
81	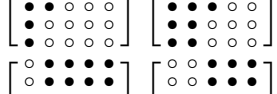						$\begin{pmatrix}1\\2\end{pmatrix}$	$\begin{pmatrix}-3\\-4\end{pmatrix}$
82	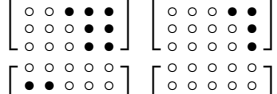						$\begin{pmatrix}2\\1\end{pmatrix}$	$\begin{pmatrix}-4\\-3\end{pmatrix}$
83	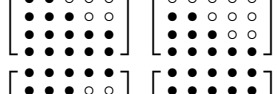						$\begin{pmatrix}2\\-1\end{pmatrix}$	$\begin{pmatrix}-4\\3\end{pmatrix}$
84	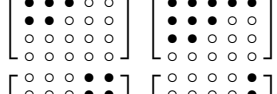						$\begin{pmatrix}1\\-2\end{pmatrix}$	$\begin{pmatrix}-3\\4\end{pmatrix}$
85	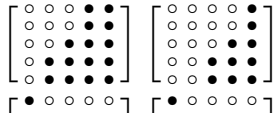						$\begin{pmatrix}1\\1\end{pmatrix}$	$\begin{pmatrix}-2\\-3\end{pmatrix}$
86	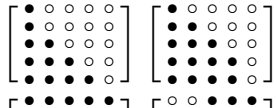		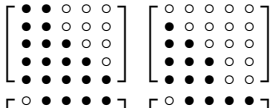				$\begin{pmatrix}2\\3\end{pmatrix}$	$\begin{pmatrix}-1\\-1\end{pmatrix}$

Table 4: The 92 groups of informative 5×5 configurations (continued).

No.	Config.	Twin	Config.	Twin	Config.	Twin	a	b
87	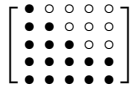	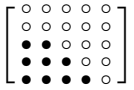	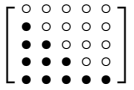	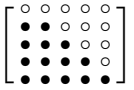			$\begin{pmatrix}3\\2\end{pmatrix}$	$\begin{pmatrix}-1\\-1\end{pmatrix}$
88	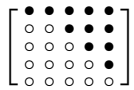	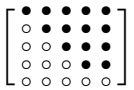	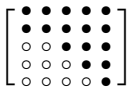	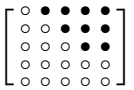			$\begin{pmatrix}1\\1\end{pmatrix}$	$\begin{pmatrix}-3\\-2\end{pmatrix}$
89	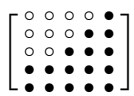	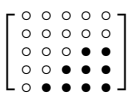	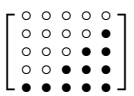	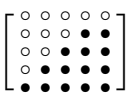			$\begin{pmatrix}1\\-1\end{pmatrix}$	$\begin{pmatrix}-3\\2\end{pmatrix}$
90	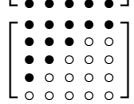	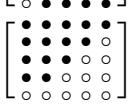	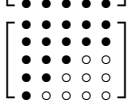	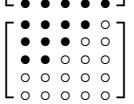			$\begin{pmatrix}3\\-2\end{pmatrix}$	$\begin{pmatrix}-1\\1\end{pmatrix}$
91	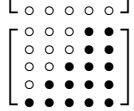	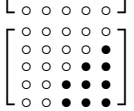	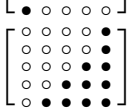	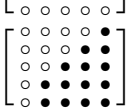			$\begin{pmatrix}2\\-3\end{pmatrix}$	$\begin{pmatrix}-1\\1\end{pmatrix}$
92	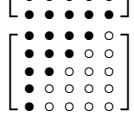	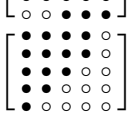	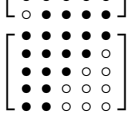	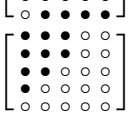			$\begin{pmatrix}1\\-1\end{pmatrix}$	$\begin{pmatrix}-2\\3\end{pmatrix}$

References

Cressie, N.A.C. (1993): *Statistics for Spatial Data*, revised edition. John Wiley & Sons, New York.

Friel, N. and Molchanov, L.S. (1999): A new thresholding technique based on random sets. *Pattern Recognition* **32** 1507–1517.

Geman, S. and Geman, D. (1984): Stochastic relaxation, Gibbs distributions, and the Bayesian restoration of images. *IEEE Transactions on Pattern Analysis and Machine Intelligence* **6** 721–741.

Greig, D., Porteous, B., and Seheult, A. (1989): Exact maximum a posteriori estimation for binary images. *Journal of the Royal Statistical Society, Series B* **51** 271–279.

Grenander, U. (1981): *Lectures in Pattern Theory*, Vol. I–III. Springer, New York.

Hartvig, N.V. and Jensen, J.L. (2000a): Spatial mixture modeling of fMRI data. *Human Brain Mapping* **11** 233–248.

Hartvig, N.V. and Jensen, J.L. (2000b): Spatial mixture modelling of fMRI data. Research Report 414, Department of Theoretical Statistics, University of Aarhus.

Jensen, E.B.V. and Kiderlen, M. (2003): Directional analysis of digitized planar sets by configuration counts. *Journal of Microscopy* **212** 158–168.

Kiderlen, M. and Jensen, E.B.V. (2003): Estimation of the directional measure of planar random sets by digitization. *Advances in Applied Probability* **35** 583–602.

Osher, J. and Mücklich, F. (2000): *Statistical Analysis of Microstructures in Material Science*. John Wiley, Chichester.

Ohser, J., Steinbach, B., and Lang, C. (1998): Efficient texture analysis of binary images. *Journal of Microscopy* **192** 20–28.

Otsu, N. (1979): A threshold selection method from gray-level histograms. *IEEE Transactions on Systems, Man, and Cybernetics* **9** 62–66.

Schneider, R. (1993): *Convex Bodies: the Brunn-Minkowski Theory*. Cambridge University Press, Cambridge.

Schneider, R. and Weil, W. (2000): *Stochastische Geometrie*. Teubner, Stuttgart.

Serra, J. (1982): *Image Analysis and Mathematical Morphology*. Academic Press, London.

Winkler, G. (1995): *Image Analysis, Random Fields and Dynamic Monte Carlo Methods*. Springer, Berlin.

Woolrich, M.W., Behrens, T.E.J., Beckmann, C.F., and Smith, S.M. (2005): Mixture models with adaptive spatial regularization for segmentation with an application to fMRI data. *IEEE Transactions on Medical Imaging* **24** 1–11.